Available online at www.sciencedirect.com
ScienceDirect
Optik 121 (2010) 68–76
Optik Optics
www.elsevier.de/ijleo

Performance evaluation of path-averaged soliton pulses in loss-managed 10-Gbps soliton transmission link over a long haul

Manoj Kumar[a,1], Ajay K. Sharma[b,*], T.S. Kamal[c]

[a]DAV Institute of Engineering and Technology, Jalandhar 144008, Punjab, India
[b]National Institute of Technology (Deemed University), Jalandhar 144011, Punjab, India
[c]Sant Longowal Institute of Engineering and Technology, Longowal 148106, Punjab, India

Received 26 December 2007; accepted 27 May 2008

Abstract

In this paper, the performance evaluation of path-averaged soliton transmission link for various performance measures viz. OSNR, optical power, extinction ratio, bit error rate (BER) and Q factor at different levels of noise figure and values of pulse width (FWHM) has been carried out. The performance of soliton transmission link is studied, taking into account soliton interaction, amplified spontaneous emission (ASE) noise and noise figure. The model presented considers interaction in a random sequence of solitons and the effect of the ASE noise added in each amplification stage. The influence of ASE noise, noise figure and pulse width with different amplifier spacing on the BER and quality factor has been investigated. It has been shown that these play dominant roles in degrading the performance measures. We have demonstrated the capability of path-averaged (guiding-centre) soliton for a long-haul distance of 17,000 km at a bit rate of 10 Gbps without ASE effect and noise figure in each amplifier span length of 500 km. The average value of quality factor is found to be 16.6 dB and the average BER is of the order of 10^{-12} over the transmission distance of 17,000 km. Further, it has been investigated that a severe system penalty results on the inclusion of ASE effect and noise figure in order to achieve the same level of performance. Thus, the investigations ascertain that in order to maintain the same level of BER and Q factor, the amplifier spacing and total transmission distance reduce considerably.

Keywords: Path-averaged soliton; Long haul; Timing jitter; BER; Q factor

1. Introduction

Soliton communication systems are leading candidates for long-haul light wave transmission links. One normally thinks of the soliton as involving dynamic balance along its path between the dispersive and non-linear terms of the non-linear Schrödinger equation. The ideal soliton can exist in a lossless fiber with a balance between the chirp induced by fiber GVD and fiber non-linearity characterized by self-phase modulation (SPM). In a real fiber, the fiber attenuation $\alpha \neq 0$ and would produce the soliton broadening simply because a reduced peak power weakens the SPM effect necessary to counteract the GVD. Thus at first it was natural to assume that distributed amplification, allowing for

*Corresponding author.
E-mail addresses: mk_daviet@rediffmail.com (M. Kumar), sharmaajayk@nitj.ac.in (A.K. Sharma).
[1]Tel.: +91 181 2200126; fax: +91 181 2207650.

0030-4026/$ - see front matter © 2008 Elsevier GmbH. All rights reserved.
doi:10.1016/j.ijleo.2008.05.017

nearly uniform cancellation of loss, would be necessary for long distance soliton transmission [1,2]. Indeed, the Raman effect, which turns silica fiber into its own distributed amplifier, enabled the first experimental studies of such transmission [3–5]. But with the recent and rapid development of the more practical EDFAs, the question immediately arose, are solitons somehow amenable to transmission through a chain of lumped amplifiers? The principle concept that has emerged in the context of lumped amplification is the path-average or guiding-centre soliton [6,7]. In [6], it has been shown both through analysis and numerical simulations that solitons can maintain their shape in periodically amplified fiber link if amplifier spacing L_A is kept smaller than the fiber dispersion length L_D. Then the non-linear effect accumulated over each L_A is simply determined by the corresponding path-average power. We can then balance the average dispersion with the average non-linear phase shift by adjusting the launched power. Thus the soliton peak power should be adjusted by a factor defined by path-averaged power. This is the concept of path-averaged soliton. Thus by keeping the path-average power constant and equal to the usual soliton power from one period to the next, one can have a perfectly well-behaved soliton.

However, the limitation that $L_A < L_D$ results in unreasonably short amplifier spacing at high bit rates. This limitation comes from the fact that the system is not perfectly periodic when L_A becomes comparable to or exceeds L_D. As a result large perturbations generate spectral side bands and dispersive radiation that degrade the system performance [8–10].

In a long-haul soliton communication system, although lumped amplifiers compensate for fiber losses but the amplification process is accompanied by the emission of spontaneous noise. The noise that is outside the bandwidth of the optical signal can be removed, using an appropriate filter, although it is not possible to remove in-bound noise. This noise co-propagates with the signal. The noise added to the signal by each amplifier induces an uncertainty in the soliton arrival time called jitter. Gordon and Haus showed that the statistics of the jitter due to spontaneous emission noise added by the lumped amplifiers is Gaussian with a variance proportional to the cube of the total distance of the links [11]. Recent experiments have shown significant deviations from the Gaussian distribution [12]. It was pointed out in [13] that soliton interaction, acoustic affects and polarization mode dispersion can lead to deviations from the Gordon–Haus results. However, the soliton interaction is likely to have the dominant effect for high bit rate systems. Further, the performance of first- and second-order path-averaged soliton long-haul transmission link has been investigated in [14] including the impact of third-order dispersion (TOD) at varied chirp. The observations establish that the pulse width (FWHM) remains within the optimal range without and up to certain discrete values of the chirp factor.

Here, the performance of path-averaged soliton transmission link for various performance measures viz. optical signal-to-noise ratio (OSNR), optical power, extinction ratio, bit error rate (BER), BER with forward error correction (FEC) and Q factor at different levels of noise figure and pulse width (FWHM) has been reported. The influence on the BER and quality factor has been investigated at bit rate of 10 Gbps without and with amplified spontaneous emission (ASE) effect and noise figure at different amplifier spacing. The results have been reported in both the cases for maintaining the average quality factor and BER of the order 16.6 dB and 10^{-12}, respectively.

After introduction in Section 1, Section 2 presents the performance measures. Section 3 details the system description. The results are discussed in Section 4 and the final conclusions are summarized in Section 5.

2. Performance measures

Long-haul transmission links experience performance degradations due to ASE-noise from optical amplifiers along the line. In transoceanic systems, a large number of amplifiers are cascaded; each of them adds noise onto the signal stream. Besides changing the pulse energy, ASE-noise affects the pulse position in non-linear pulse propagation as well. To maintain a safe pulse separation, the pulse width needs to be reduced and peak powers increased, when the channel bit rate is increased. The most widely used performance measures for performance evaluation are the OSNR, Q-factor and BER.

Q-factor represents the signal-to-noise ratio at the receiver decision circuit in voltage or current unit [15]. Fig. 1 shows the Q-factor definition. This definition considers soliton stability, interactions between pulses, timing jitter effects and other effects. In soliton-based systems using relatively higher signal power, we can use relatively short bit patterns because the stability of

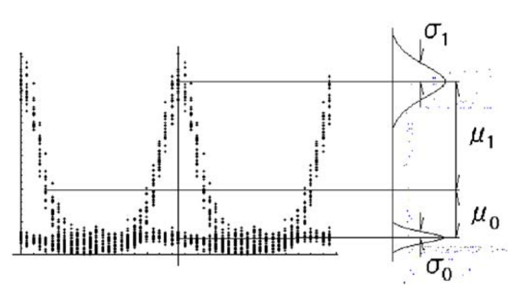

$$Q = \frac{\mu_0 + \mu_1}{\sigma_0 + \sigma_1}$$

σ : standard deviation
μ : mean value

Fig. 1. Q-factor definition.

soliton pulses and non-linear interactions between adjacent pulses are dominant compared to the pulse pattern effects and signal to noise ratio.

The BER can be estimated from Eq. (1), and requires $Q > 6$ for the BER of 10^{-9}. This BER gives the upper limit for the signal because some degradation occurs in the de-multiplexing circuit:

$$\mathrm{BER} = \frac{1}{2}\mathrm{erfc}\left(\frac{Q}{\sqrt{2}}\right) \approx \frac{\exp(-Q^2/2)}{Q\sqrt{2\pi}} \quad (1)$$

3. System description

Soliton pulses by nature exhibit many desirable properties making them suitable for use in long-haul communication systems. Relying on the balance between non-linearly induced SPM and dispersion, these pulses are capable of maintaining their shapes over large distances. Here we define the soliton pulse profile as

$$S(t) = N \ \sec h[\tau T_0], \quad (2)$$

Fig. 2 shows the simulation model system block diagram. It demonstrates the layout of path-averaged soliton regime for soliton pulses passing through a chain of amplifiers forming loss-managed soliton link with 10-Gb/s modulated signal. Here, the amplifier gain is considered as $G = \exp\ (\alpha L_A)$, then the enhancement factor for loss-managed soliton can be derived as

$$f_{LM} = \left[\frac{1}{L_A}\int_0^{L_A} \exp(-\alpha z)\,dz\right]^{-1} = \frac{\alpha L_A}{1-\exp(-\alpha L_A)} = \frac{G \ln G}{G-1} \quad (3)$$

Fig. 2 describes the optical soliton loss-managed long-haul transmission link of 17,000 km with 34 amplifiers inserted after every 500-km span of a dispersion-shifted fiber (DSF) without including ASE effect in each amplifier spacing and noise figure. The PRBS generator generates a binary sequence of data stream. The electrical signal generator converts an input binary signal into an output electrical signal. The transmitter is set up as a train of optical pulses and the pulse source is a mode-locked laser generating pulses of "sech" shape with specified power and width. It consists of an optical source, which generates fundamental soliton pulses ($N = 1$). The pulses are then modulated by data at 10 Gb/s bit rate.

The re-circulating loop includes a 500 km long DSF and an EDFA. In order to compensate for the power loss during solition pulse propagation, the attenuated soliton pulses are amplified and as a result they undergo an adjustment period where the pulse width adapts itself. During this period, the solitons lose some of their energy as dispersive waves. The effect of these potentially hazardous waves crucially relies on the relationship between the loss per dispersion length L_D and the amplifier period L_A. The dispersion length L_D is given as

$$L_D = \frac{T_0^2}{|\beta|} \quad (4)$$

If both $L_D \ll 1$ and $L_A \gg L_D$, the amplification regime is termed quasi-adiabatic. In this regime, the soliton is capable of adjusting itself to the energy loss adiabatically. Conversely, when $L_A \ll L_D$, the modus operandi is referred to as the average soliton regime. Here the soliton shape is not distorted significantly despite the energy loss and the pulses may consequently be amplified hundreds of times. The main disadvantage is that the relatively close amplifier spacing makes it unsuitable for long-haul high-bit rate ($\geqslant$20 Gb/s) communications.

A spectrum analyzer at the end of the re-circulating loop gives the output power spectrum. In our system set-up, we have considered the fiber loss $\alpha = 0.2$ dB/km and amplifier spacing L_A is 500 km. Hence, gain $G =$ 100 dB and enhancement factor $f_{LM} = 23.03$. Second- and third-order fiber dispersion parameters are $\beta_2 = -0.2178\ \mathrm{ps^2/km}$ and $\beta_3 = 0.0745\ \mathrm{ps^3/km}$ and non-linear coefficient $\gamma = 1.75\mathrm{e}^{-31}$/m/W, input pulse width

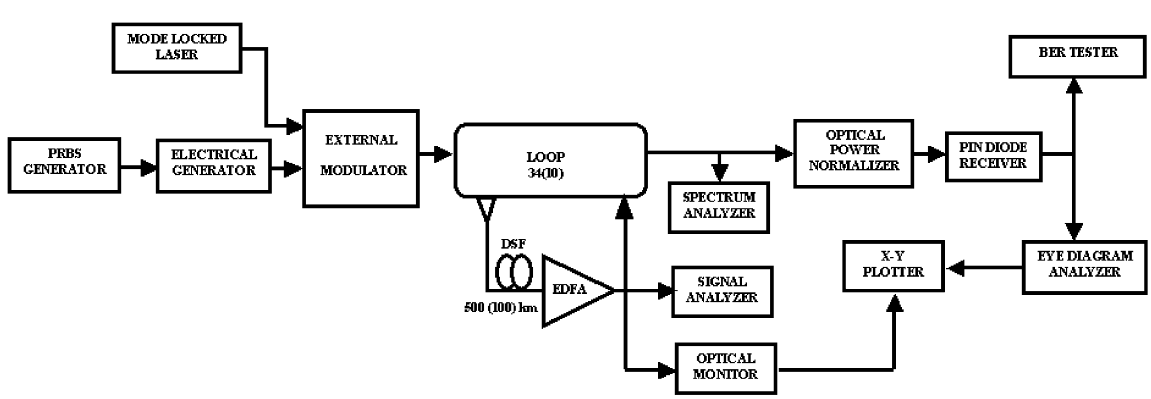

Fig. 2. Layout for path-averaged loss-managed soliton link.

$T_o = 14.18$ ps and $\lambda = 1550$ nm will provide second- and TOD lengths as

$$L_{D_{\beta_2}} = \frac{T_0^2}{|\beta_2|} \approx 923\,\text{kms}, \quad L_{D_{\beta_3}} = \frac{T_0^3}{|\beta_3|} \approx 38297\,\text{kms} \tag{5}$$

and soliton peak power $P_o = 6.197$ mW. The launched peak power will be $P_o' = f_{LM} \times P_o$, thus soliton evolution in lossy fibers with periodic lumped amplification is identical to that in lossless fibers with launch power P_o' providing $L_A < L_D$. The dominant non-linear fiber parameters considered during simulation are the Kerr non-linearity coefficient:

$$\gamma = \frac{n_2 \omega_0}{c A_{eff}} \tag{6}$$

For the fixed values of non-linear refractive index:

$$n_2 = 2.6 \times 10^{-20}\,\text{m}^2/\text{W},$$
$$\omega_0/c = 2\pi/\lambda = 2\pi/1.55 \times 10^{-6}\,\text{m}^{-1},$$
$$A_{eff} = 60.31\,\mu\text{m}^2 \tag{7}$$

The re-circulating loop is terminated in the optical receiver followed by the BER tester and the eye diagram analyzer. Prior to receiver, the optical power normalizer has been configured, which normalizes the optical signal power by attenuating the input optical signal to the specified average output power level. This is most often used to control the input optical power at the receiver when preparing a BER vs. received optical power curve plot. The optical power normalizer attenuates all input optical signals to the same average output power regardless of their different average input powers, or it is used to attenuate all input optical signals by the same amount such that the signal with the largest average input power has the specified average output power. In our set-up, we have configured the optical power normalizer for uniform attenuation at −25 dBm.

NRZ format was used here in the electrical signal generator since it requires less bandwidth both for the transmitter as well as the receiver. The modulation format impacts the design of a given link; each stage of optical amplification introduces noise due to ASE of optical amplifiers. As a result, the OSNR degrades along the link. An empirical expression for OSNR is given by the following equation:

$$\text{OSNR} = 58 - 10 \times \log(N) - \text{NF} - 10\log(L) + P_{out} - 10 \times \log(M) - k \tag{8}$$

where M = number of channels, N = number of amplifiers, L = loss/span, NF = noise figure of amplifier, P_{out} = amplifier output power and k = other factors.

The BER tester computes the BER for the input electrical signal(s) as well as a number of useful parameters such as the Q factor and electrical eye properties such as the height, width, area and extinction ratio. The BER may be calculated using either a quasi-analytical or Monte-Carlo algorithm depending on the nature of the dominant noise sources in the simulation.

The BER of a fiber link is the most important measure of the faithfulness of the link in transporting the binary data from the transmitter to the receiver. From time to time, due to signal degradations from dispersion, non-linearities and noise, a signal is so distorted that the detector makes a mistake – a binary one or "mark" is recorded where a binary zero or "space" was transmitted. Clearly, if the link is to be of any use, the frequency of such errors must be as small as possible. The BER quantifies the rate of errors and is defined as the probability of an error occurring per transported bit. Typical benchmarks for the BER are rates of 10^{-9} and 10^{-12}, though with the use of FEC codes, much lower rates can be acceptable.

A pseudo-random bit source modulating the source is also connected to the BER testing apparatus and the binary value of every transmitted bit is compared against the value of the same bit at the receiver. For a 10 Gbps system, a BER near 10^{-9} can be measured in a few seconds, while rates near 10^{-12} can be measured in hours. But in the *OptSim* simulation tool used by us, it involves hundreds to thousands or perhaps tens of thousands of bits and if the link is long or the simulation challenging a single run may take minutes or even hours. To establish a BER of 10^{-12} by direct counting of errors – a technique sometimes known as Monte-Carlo simulation – would require the simulation of trillions of bits, which is clearly out of the question. Instead of this direct approach, numerical tools attempt to extrapolate an estimate of the BER from simulation of just hundreds or thousands of bits. If the BER is acceptable, then it is very unlikely that an "error bit" will actually occur within the simulation time window, but by measuring the shape of the received electrical eye, the simulator can extract basic parameters describing the distribution of bits and produce a BER estimate with confidence limits.

Further, the computer simulation model of the system block diagram shown in Fig. 2 was remodeled to include the impact of ASE effect and noise figure on the system and the investigations were carried out to evaluate the system performance by measuring OSNR, optical power, extinction ratio, BER and Q factor.

4. Results and discussion

In order to simulate the propagation behavior, it is preferable to operate near the soliton regime where there is relatively little shedding of dispersive energy. The results have been obtained at bit rate $B = 10$ Gb/s, $T_{FWHM} = 25$ ps and bit pattern length of seven bits, which is preceded by two bits and followed by three bits generating a sequence length of 12 bits. In this work, the impact on bit stream at different span lengths over a long-haul soliton transmission link of 17,000 km without including the ASE effect in each amplifier spacing and noise figure has been analyzed, which show the robustness of path-averaged soliton pulses up to a transmission distance of 17,000 km. We have also studied the impact of ASE effect and noise figure on the system and it has been investigated that the amplifier spacing and total transmission distance because of ASE noise and interaction between adjacent pulses decrease considerably. It has been investigated that a severe system penalty results on the inclusion of ASE effect and noise figure in order to achieve the same level of performance. Thus amplifier spacing and in turn total transmission distance had to be cut down considerably in order to meet same level of performance (BER and Q factor) that was achieved without consideration of ASE effect and noise figure. In the later case, amplifier spacing was reduced to 100 km and with inclusion of 10 EDFAs wherein one EDFA was inserted after every span of 100 km long DSF restricting total transmission distance up to 1000 km. Further, the results have been obtained for various performance measures viz. OSNR, optical power, extinction ratio, BER and Q factor at different levels of noise figure and values of pulse width (FWHM) to carry out the performance evaluation of path-averaged soliton transmission link.

Fig. 3(a) shows the optical bit stream of soliton input signal at the input end of the fiber using an signal analyzer (not indicated in the block diagram) and Fig. 3(b) shows the input power spectrum observed using the spectrum analyzer. Fig. 4 shows the resulting optical bit stream of path-averaged soliton pulses modulated at 10 Gb/s by the mode locked laser using external modulator at the fiber output. The envelope of modulated output signal at a transmission distance of 5000, 10,000, 15,000, 17,000 and 20,000 km is shown in Fig. 4 from (a) to (e). A very little distortion in the output signal because of interaction between adjacent pulses up to the transmission distance of 17,000 km is observed as depicted in Fig. 4(a)–(d). Fig. 4(f) shows the output power spectrum observed at the end of fiber output at a transmission distance of 17,000 km, which very well maps with input power spectrum of Fig. 3(b).

It is clearly seen that two adjacent pulses move toward each other as they propagate, whereas the short pulsewidth and high optical OSNR are maintained. Therefore, it is concluded that transmission distance is mainly limited by the soliton interaction. This demonstrates the robustness of path-averaged soliton pulses over a long-haul transmission system that are able to maintain their integrity, as the shape and width of the pulses does not change (Fig. 4(a)–(d)).

The results obtained in Fig. 4 are well supported by the receiver eye diagram as shown in Fig. 5(a) and

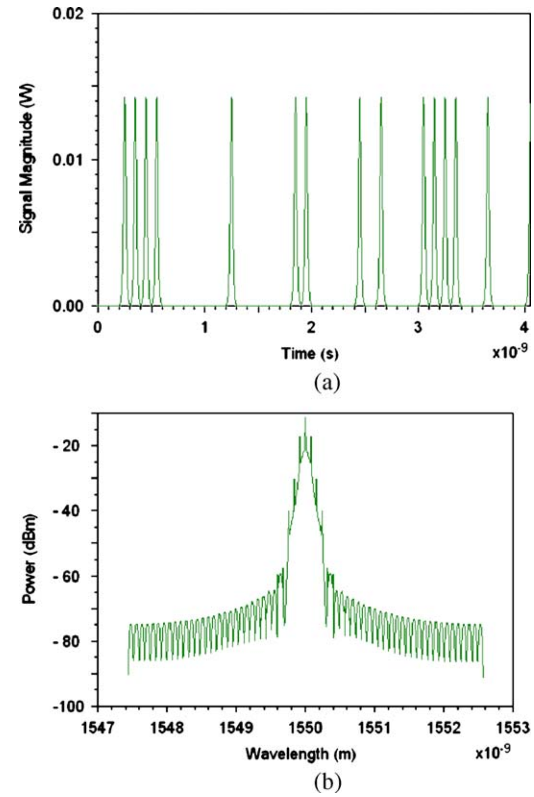

Fig. 3. Path-averaged soliton modulated at 10 Gb/s; (a) signal at the fiber input, (b) input power spectrum.

decision level offset of lower and upper lids as observed in Fig. 5(b), it is wide open and provides error-free communication. Further, as the transmission distance is increased to 20,000 km and above as shown in Fig. 4(e), it is observed that because of increased interaction between the soliton pulses due to further increase in transmission distance and at transmission rate of 10 Gb/s, the amplitudes of the pulses vary because of exchange/transfer of energy between them and the pulses broaden and merge together because of increased soliton–soliton interaction contributing timing jitter and thus results in increased BER. The BER observed at 20,000 km is very high and it is of the order of 10^{-2} and the degradation of Q factor occurs due to pulse broadening.

The system performance is measured by obtaining the quality factor; Q^2 (dB) value of the transmitted signal. Q factor of six corresponds to Q^2 (dB) value of 15.6. In this case, Q^2 (dB) value is measured to be ranging from 16.2 to 17 dB and the average value of Q^2 (dB) value is found to be 16.6 dB and the average BER is measured to be of the order of 10^{-12}, which is exceptionally good for a soliton transmission link.

The results have been obtained for various performance measures viz. OSNR, optical power, BER, BER with FEC and quality factor at different levels of noise figure varying from NF = 3 to 6 and ASE noise as

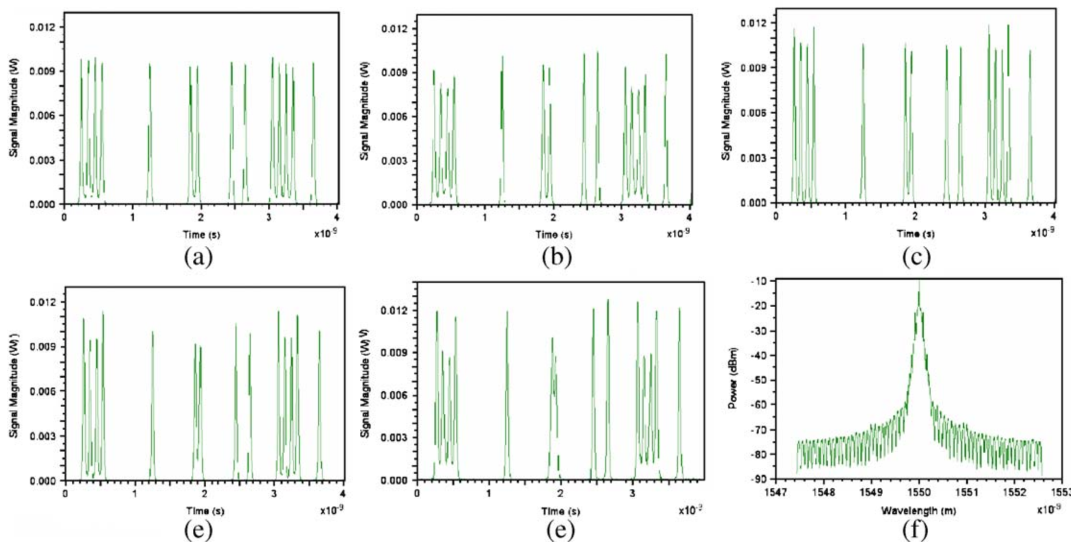

Fig. 4. 10 Gb/s modulated output at a transmission distance of (a) 5000 km, (b) 10,000 km, (c) 15,000 km (d) 17,000 km, (e) 20,000 km and (f) output power spectrum.

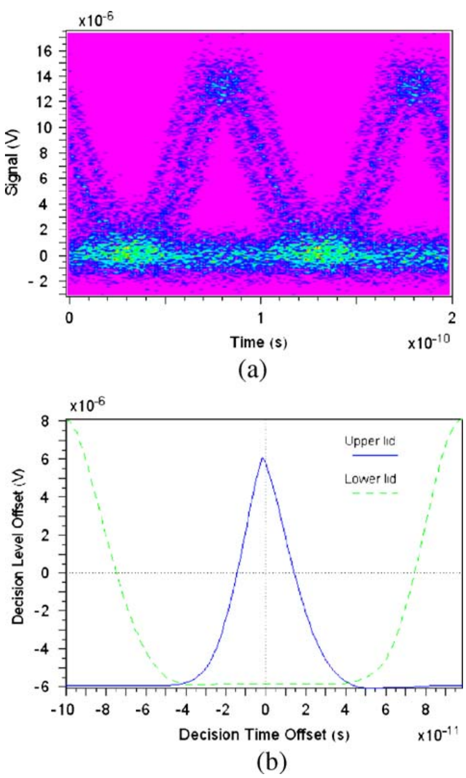

Fig. 5. Received signal at a transmission distance of 17000 km without taking into account ASE noise, noise figure and timing jitter. (a) Eye diagram, (b) decision level offset of lower and upper lids.

shown in Fig. 6(a)–(e). Fig. 6(a) shows the results for OSNR vs. amplifier spacing at different levels of NF. It has been obtained that OSNR penalty increases with increase in NF. The best results are reported at NF = 3 and OSNR of 18 dB has been achieved with this noise figure level over the span length of one amplifier spacing measuring 100 km. Fig. 6(b) and (c) shows the plots for Q^2 (dB) vs. amplifier spacing (L_A) and optical power strength vs. Q^2 (dB), respectively. In the simulations that we carried out, Q^2 (dB) value of 16.5 dB was achieved over the amplifier span length of 100 km. Fig. 6(b) shows that Q factor degraded linearly with transmission distance over one amplifier spacing, which indicates that the fiber non-linearity was well suppressed. This tendency indicates that Q factor degradation is mainly due to SNR and that the waveform distortion and timing jitter are quite small. Further, it was obtained in Fig. 6(c) that optical power reduces sharply as the quality factor Q^2 increases beyond 17 dB. In our system modeling, no optical band pass filters were used at the end of EDFAs, keeping in view the economic aspect of commercial viability of this system.

In a long-haul transmission system, FEC is particularly important to enhance the system margin and to increase the transmission distance and the repeater spacing. Basically, the higher the FEC redundancy i.e., the higher the line rate, the larger the net FEC gain. For 10 Gb/s applications, more than 14–20% redundancy has been used [16]. In Fig. 6(d) and (e), the results have been obtained for BER and BER with FEC vs. amplifier spacing at varied levels of noise figure. BER of the order of 10^{-13} was obtained up to a transmission distance of 100 km over one amplifier spacing at NF = 3 and it reduces marginally as the noise figure increases up to 6. As shown in Fig. 6(e), our investigations reveal that by employing FEC, a uniform level of BER with FEC can be achieved throughout the length of one amplifier spacing at all levels of noise figure ranging from NF = 3 to 6.

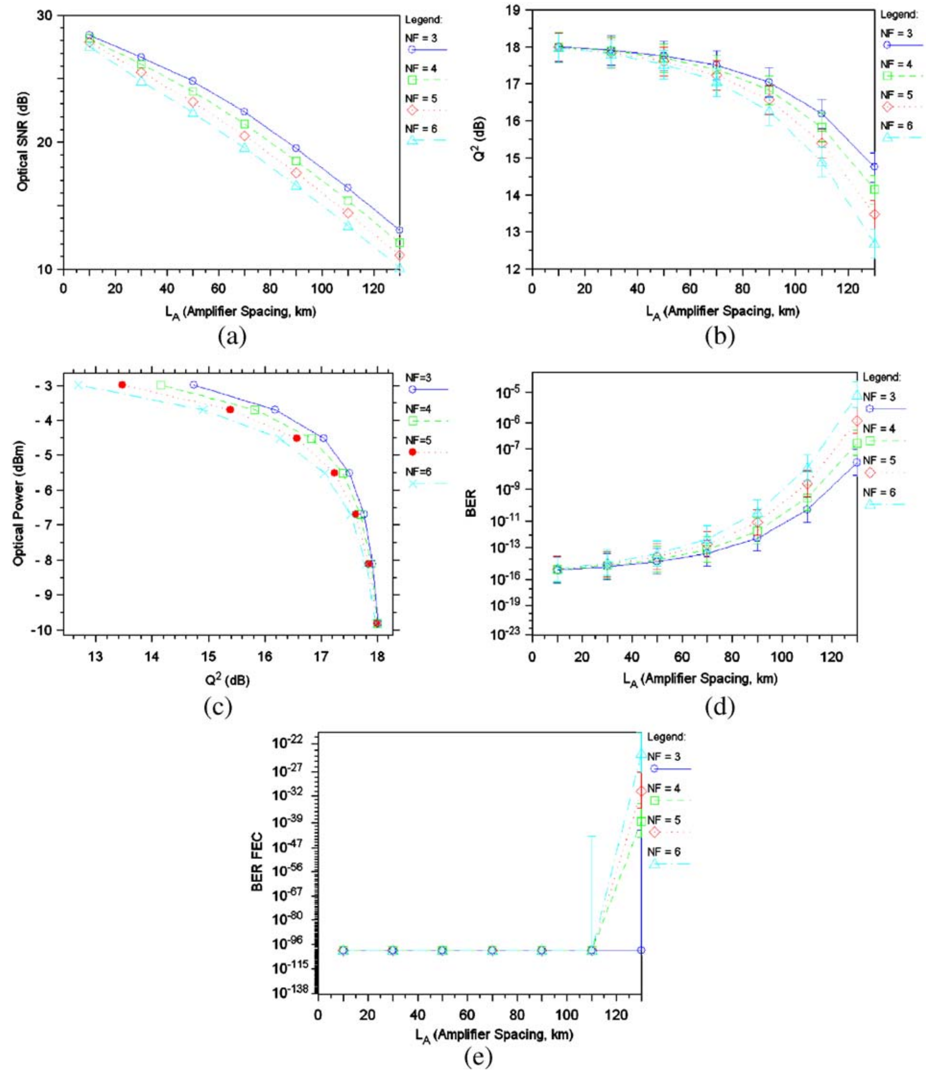

Fig. 6. Performance measures along the length of one amplifier spacing at different levels of noise figure and ASE noise (a) OSNR vs. L_A, (b) Q^2 (dB) vs. L_A, (c) optical power vs. Q^2 (dB), (d) BER vs. L_A and (e) BER with FEC vs. L_A.

The results were also obtained for various performance measures viz. OSNR, optical power, extinction ratio and Q factor at different values of pulse width (FWHM) varying from FWHM = 5 to 55 ps as shown in Fig. 7(a)–(d). Fig. 7(a) shows the results for OSNR vs. amplifier spacing at different values of FWHM. It is obtained that OSNR remains constant at a value of 18.5 dB up to a transmission distance of 90 km over one length of an amplifier spacing, measuring span length of 100 km. For ultra short pulses of FWHM = 5 and 15 ps, OSNR value lies within 6–18 dB up to 100 km, while for pulses with higher FWHM ranging from 25 to 55 ps, it has been observed that the OSNR value decreases linearly from high initial value of 30 to 18 dB with relative decrease in OSNR at higher values of FWHM. Fig. 7(b) shows the plots for optical power strength vs. amplifier spacing (L_A). It is obtained that the optical power level is highest for ultra short optical pulse width (FWHM = 5 ps) and it decreases for higher values of pulse widths. Extinction ratio is another important performance measure in a transmission system. Fig. 7(c) shows the results obtained for extinction ratio vs. amplifier spacing at different values of FWHM. It is obtained that the extinction ratio is highest for pulse width with FWHM = 15 and 25 ps resulting in an extinction ratio of the order of 34 dB. However, for ultra short pulses with FWHM = 5 ps, it decreases sharply and it reduces to 4 dB at a distance of 100 km along the amplifier span length. Fig. 7(d) shows the plots for quality factor Q^2 (dB) vs. amplifier spacing at different values of FWHM. It is obtained in Fig. 7(d) that a high value of Q factor ranging from 15 to 20 dB results and it remains fairly constant along the amplifier span length of 100 km at all values of pulse width (FWHM = 5–55 ps).

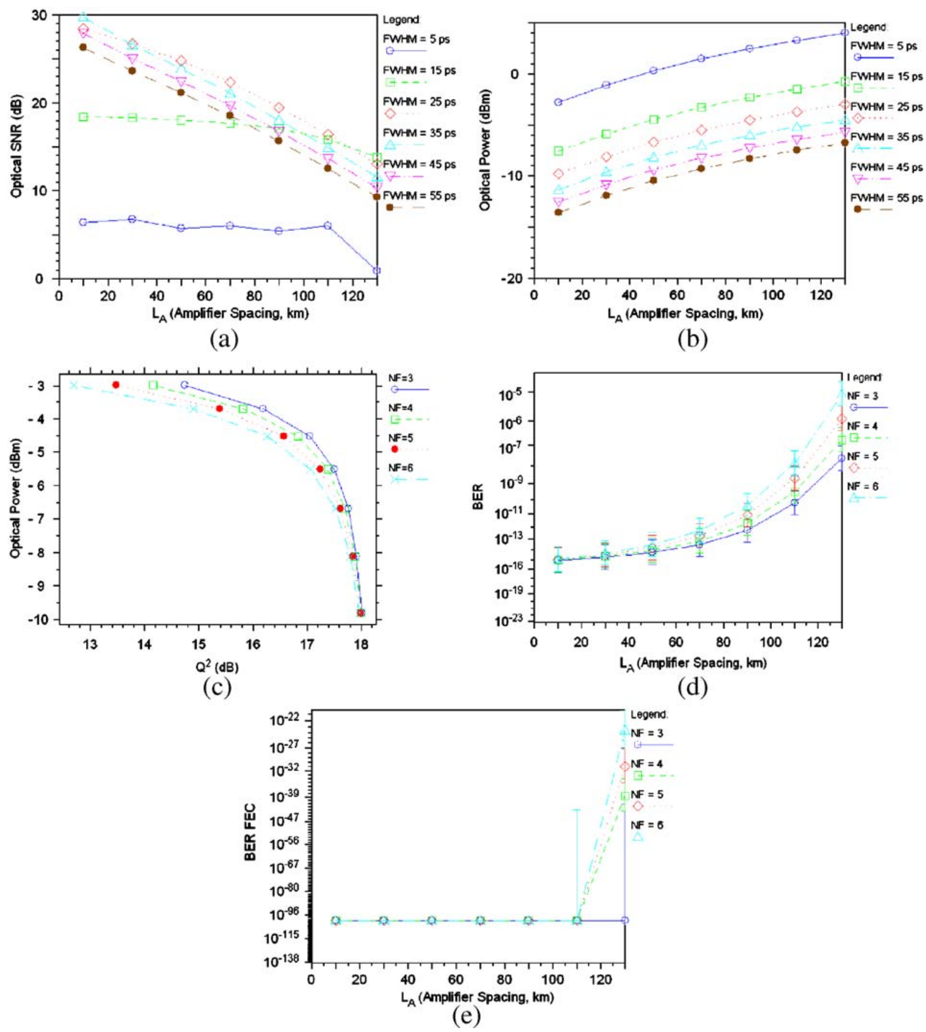

Fig. 7. Performance measures along the length of one amplifier spacing at different values of pulse width (FWHM). (a) OSNR vs. L_A, (b) optical power vs. L_A, (c) extinction ratio vs. L_A, (d) Q^2 (dB) vs. L_A and BER FEC vs. L_A.

5. Summary of conclusions

In summary of conclusions, we have presented results that demonstrate a maximum transmission distance of 17,000 km at 10 Gbps channel over DSF, which we believe to be the best reported to date, achieved with path-averaged soliton with higher-order dispersion parameters and without any dispersion management and soliton control technique. We have demonstrated the capability of path-averaged (guiding-centre) soliton for a long-haul distance of 17,000 km at bit rate of 10 Gbps without and with ASE effect and noise figure. The average value of quality factor is found to be 16.6 dB and the average BER is of the order of 10^{-12} over the transmission distance of 17,000 km. It has been investigated that a severe system penalty results on the inclusion of ASE effect and noise figure in order to achieve the same level of performance. The total transmission distance, amplifier spacing, BER and quality factor reduce considerably.

The use of FEC in particular is important to enhance the system margin and to increase the transmission distance and the repeater spacing. Here, the results have been obtained for BER and BER with FEC vs. amplifier spacing at varied levels of noise figure and ASE noise. Our investigations divulge that by employing FEC, a uniform level of BER with FEC has been achieved throughout the length of amplifier spacing at all levels of noise figure ranging from NF = 3 to 6. Moreover, for ultra short pulses of FWHM = 5 and 15 ps, OSNR value lies within 6 and 18 dB, respectively, over amplifier span length of 100 km, while for pulses with higher FWHM ranging from 25 to 55 ps, it has been observed that the OSNR value decreases linearly from high initial value of 30–18 dB with relative decrease in OSNR at higher FWHM.

References

[1] A. Hasegawa, Amplification and reshaping of optical solitons in glass fiber-IV, Opt. Lett. 8 (1983) 650–652.

[2] L.F. Mollenauer, J.P. Gordon, M.N. Islam, Soliton propagation in long fibers with periodically compensated loss, IEEE J. Quantum Electron. QE-22 (1986) 157–173.

[3] L.F. Mollenauer, K. Smith, Demonstration of soliton transmission over more than 4000 km in fiber with loss periodically compensated by Raman Gain, Opt. Lett. 13 (1988) 675–677.

[4] K. Smith, L.F. Mollenauer, Experimental observation of adiabatic compression and expansion of soliton pulses over long fiber paths, Opt. Lett. 14 (1989) 751–753.

[5] K. Smith, L.F. Mollenauer, Experimental observation of soliton interaction over long fiber paths: discovery of long-range interaction, Opt. Lett. 14 (1989) 1284–1286.

[6] Linn F. Mollenauer, Stephen G. Evangelides, Hermann A. Haus, Long-distance soliton propagation using lumped amplifiers and dispersion shifted fiber, J. Light Wave Technol. 9 (2) (1991) 194–197 February.

[7] A. Hasegawa, Y. Kodama, Guiding centre-soliton in optical fibers, Opt. Lett. 15 (1990) 1443–1445;
A. Hasegawa, Y. kodama, Guiding centre-soliton in optical fibers, Phys. Rev. Lett. 66 (1991) 161–164.

[8] S.M.J. Kelly, Characteristic side band instability of periodically amplified average soliton, Electron. Lett. 28 (1992) 806–807.

[9] N.J. Smith, K.J. Blow, I. Andonovic, Sideband generation through perturbations to the average soliton model, J. Lightwave Technol. 10 (1992) 1329–1333.

[10] J.P. Gordan, Dipersive perturbations of solitons of the nonlinear Schrödinger equation, J. Opt. Soc. Am. B 9 (1992) 91–97.

[11] J.P. Gordan, H.A. Haus, Random walk of coherently amplified solitons in optical fiber transmission, Opt. Lett. 11 (10) (1986) 665–667.

[12] L.F. Mollenauer, P.V. Mamyshev, M.J. Neubelt, Measurement of timing jitter in filter-guided soliton transmission at 10 Gbits/s and achievement of 375 Gbits/s-Mm, error free at 12.5 and 15 Gbits/s, Opt. Lett. 19 (10) (1994) 704–706.

[13] C.R. Menyuk, Non-Gaussian corrections to the Gordon–Haus distribution resulting from soliton interactions, Opt. Lett. 20 (3) (1995) 285–287.

[14] M. Kumar, Ajay K. Sharma, T.S. Kamal, Significance of prechirping on long-haul path-averaged soliton impulse in re-circulating loop at 10 and 20 Gb/s with TOD, Opt. Int. J. Light Electron. Opt. (2007).

[15] N.S. Bergano, F.W. Kerfoot, C.R. Davidson, Margin measurements in optical amplifier systems, IEEE Photon. Technol. Lett. 5 (1993) 304–306.

[16] Mastoshi Suzuki, Noboru Edagawa, Dispersion managed high capacity ultra long haul transmission, J. Lightwave Technol. 21 (4) (2003).